RECENT PROGRESS IN UPGRADE OF THE HIGH INTENSITY THz-FEL AT OSAKA UNIVERSITY

G. Isoyama#, M. Fujimoto, S. Funakoshi, K. Furukawa, A. Irizawa, R. Kato, K. Kawase, A. Tokuchi, R. Tsutsumi, M. Yaguchi, ISIR, Osaka University, Ibaraki, Osaka 567-0047, Japan

Abstract

The THz-FEL based on the 40 MeV, L-band electron linac is working in the wavelength region from 25 to 150 μm or in the frequency region from 2 to 12 THz. For basic study on FEL physics and its applications, the linac and the FEL are upgraded to have higher stability and intensity in operation of the FEL. The high voltage power supply of the inverter type is remodelled and the solid state switch is developed in place of the thyratron for the klystron modulator, so that fractional variations of the klystron voltage are reduced from 2×10^{-4} to 8×10^{-6} (rms). As a result, fractional variations of the FEL macropulse energy are reduced to 2.4 % (rms). A new grid pulser for the thermionic electron gun of the linac is developed, which generates a series of pulses with the duration of 5 ns at intervals of 36.8 ns. Using the grid pulser, charge in an electron bunch is increased four times higher though the bunch intervals quadruple, so that the micropulse energy increases more than ten times higher than that in the conventional operation mode. The maximum micropulse energy in the new operation mode exceeds 0.1 mJ/micropulse at wavelengths around 70 μm (4.3 THz). Application experiments have begun using the high intensity and stable FEL beam.

INTRODUCTION

We have been conducting a free-electron laser based on the L-band electron linac at the Research Laboratory for Quantum Beam Science of the Institute of Scientific and Industrial Research (ISIR), Osaka University. The first lasing was achieved in 1994 at wavelengths from 32 to 40 μm. We then began remodelling the FEL to expand the wavelength region towards the longer wavelength side and obtained lasing at 150 μm or 2 THz in 1998 [1], which was the longest wavelength at that time obtained with FELs based on RF linacs. However, the intensity of the FEL was not high enough to reach the power saturation level and its stability was low because the linac was constructed in 1970s and not for FEL. We had an opportunity to upgrade the linac for higher stability and reproducibility in operation in 2003. In doing so, we have added a new operation mode for FEL, in which the RF pulse duration is increased from 4 μs for the standard operation mode to 8 μs, and the number of amplifications is increased not twice but three times higher because the first 2 μs part of the electron pulse is lost in the FEL beam line owing to an energy variation there generated by the filling time of the RF power and the onset of the beam loading in the acceleration tube of the linac. As a result, the FEL is operated in the high intensity reaching power saturation and operational stability is significantly improved [2].

We have been upgrading the THz-FEL further. In this paper, we will report results of the recent progress of the FEL in stability and power.

STABILIZATION

The stability of the FEL output power is crucial for basic study on FEL and its applications. It depends strongly on stability of the linac and hence all the possible measures at that time were taken in the previous remodelling of the linac. Nevertheless, the macropulse energy of FEL fluctuated by some tens of a percent. Crucial parameters for the linac stability are the RF power and its phase provided to the 1.3 GHz RF structures, including the pre-buncher, the buncher, and the 3 m long acceleration tube. These parameters strongly depend on the voltage generated with the klystron modulator and applied to the klystron. The stability of the klystron voltage V_k is primarily determined by a high voltage power supply of the klystron modulator. The large energy

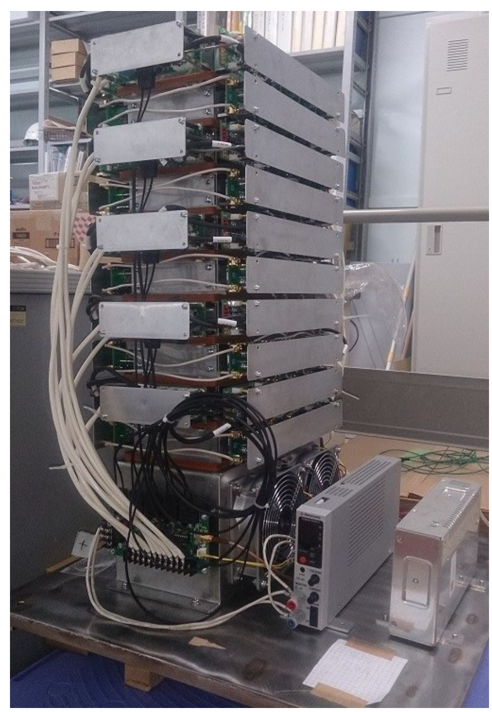

Figure 1: Solid state switch 2nd model for the klystron modulator. The maximum holding volate is 25 kV and the peak current is 6 kA for 8 μs pulses at a repetition frequency of 60 Hz.

#isoyama@sanken.osaka-university. ac.jp

Copyright © 2015 CC-BY-3.0 and by the respective authors

ISBN 978-3-95450-134-2

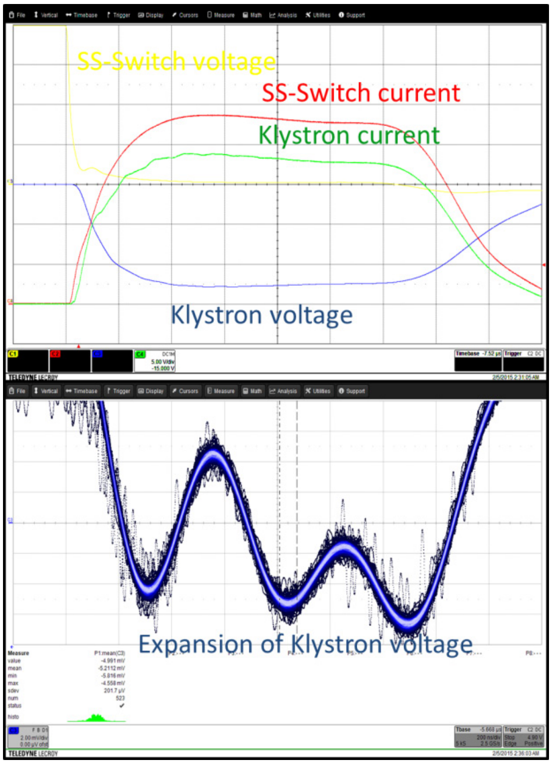

Figure 2: Voltage and current waveforms of the solid state switch and those of the klystron (upper panel) and expansion of the klystron voltage (lower panel). The klystron voltage in the lower panel is 523 pulses overlaid on the screen and its fractional variation is 8×10^{-6} (rms) or 8 ppm.

fluctuation of the FEL pulses indicates that the high voltage power supply we used is not stable enough, which is an inverter type power supply charging the PFN with fractional stability of ~10^{-3} or less. The two step charging process is employed to charge the PFN with the power supply; the coarse charging to 90 % in steps of 0.5 % and the fine charging to a target voltage by reducing the width of charging pulses. In order to make the stability higher, a new charging procedure has been developed. Instead of the pulse-width modulation circuit, a sub charging line with higher impedance is added to reduce charge per pulse, and the charging line is switched from the main line to the sub one when the PFN voltage reaches 99 % of the target value and the fine charging continues in steps of an order of 10^{-5} in the remaining part to the target value. The stability of the charged PFN voltage is measured to be 8×10^{-6} (rms), which is measured using a differential amplifier (Lecroy DA1855A). The measured value is significantly smaller than that obtained with the previous system.

The PFN is discharged using a thyratron and high voltage pulses are generated for the klystron. The fractional stability of the klystron voltage should be equal to that of the PFN voltage, but the measured stability of the klystron voltage is 2×10^{-4}, which is much larger than the stability of the PFN voltage, 8×10^{-6}. The source of the instability is considered to be the thyratron, which is a gas filled discharge tube. We have developed a solid state switch that can replace the thyratron [3]. The switch is made of sixty static induction thyristors; ten of them connected in series with six such connected in parallel. The maximum specifications of the solid state switch are a holding voltage of 25 kV and a pulse duration of 8 μs at a repetition frequency of 10 Hz, which are sufficient for operation of the linac. Figure 1 shows a photograph of the second model of the solid state, which is improved compared to the first model in that an operation mode can be chosen by changing wirings in the switch between 25 kV/6 kA and 50 kV/3 kA to be used for common klystron modulators and that the repetition rate is increased from 10 Hz to 60 Hz by reinforcement of the air cooling system. As shown in Fig. 2, the stability of the klystron voltage is measured for the second model using the differential amplifier to be $dV_k/V_k = 7.8\times10^{-6}$, which is nearly equal to that of the high voltage power supply for PFN charging, so that the stability of the solid state switch is much higher than that of the high voltage power supply. As a result of introduction of the solid state switch, the fluctuation of the FEL macropluse energy is reduced from 5.4 % for the thyratron to 2.4 % for the solid state switch.

HIGH POWER OPERATION

In the conventional mode of linac operation for FEL, which is named the 108 MHz mode, the grid pulser for

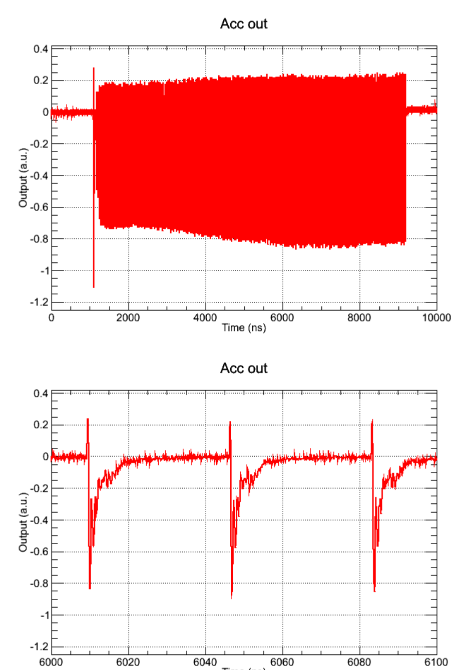

Figure 3: Electron beam current measured with a core monitor at the exit of the linac operated using the 27 MHz grid pulser. The upper panel shows the whole electron pulse of an 8 μs duration and the lower panel is its expansion showing electron bunch singals at 36.8 ns intervals.

ISBN 978-3-95450-134-2

Copyright © 2015 CC-BY-3.0 and by the respective authors

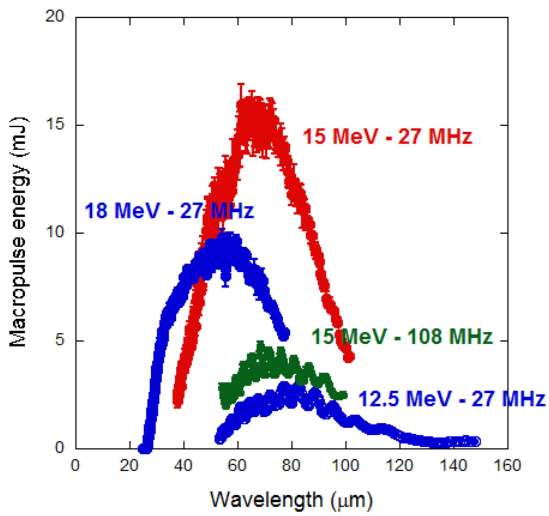

Figure 4: Macropulse energy measured with an energy meter in various operation modes at the zero detning by varying the wiggler gap.

the thermionic cathode generates 8 μs long square pulses and the electron gun generates rectangular pulses with the same duration and a peak current of 0.6 A. The second 108 MHz and the 216 MHz cavities of the three-stage sub-harmonic buncher (SHB) system are excited, so that a series of bunches, each of which has 1 nC charge, separated by 8.2 ns and continuing for 6 μs are generated at the FEL. The roundtrip time of FEL pulses in the optical cavity is 36.8 ns, so that four FEL pulses lase independently in the cavity. The electron current injected to the linac is limited by the beam loading in the acceleration tube and the current of 0.6 A in the 108 MHz mode is the maximum. In order to increase the bunch charge while maintaining the average beam current, we have developed a new grid pulser for the electron gun to generate a series of electron pulses with 5 ns duration and a peak current of 2.4 A continuing at intervals of 36.8 ns for 8 μs so that a single FEL pulse can develop in the optical cavity. The electron beam from the gun has a frequency component of 108 MHz, so that all the SHB cavities are excited to generate an electron beam with uniform energy over 6 μs for FEL. Figure 3 shows the electron beam measured at the exit of the linac using a core monitor and its expansion in time. The new

Table 1: Main Parametrs of the THz-FEL

Wavelength/Frequency range	25~150 μm/2~12 THz
Repetition frequency	10 Hz
Macropulse length	3 ~ 4 μs
Micropulse length	< 20 ps
(High power mode / Conventional mode)	
Macropulse energy	10~27 / 3~10 mJ at 70~80 μm
Micropulse intervals	36.8 / 9.2 ns
Micropulse energy	100~260 / 10~30 μJ

operation mode of the linac named the high power mode or the 27 MHz mode is successfully commissioned and electron bunches with charge of 4 nC/bunch continuing at intervals of 36.8 ns for 8 μs are generated and transported to the FEL [4].

The FEL is successfully operated in the 27 MHz mode at an electron energy of 15 MeV. As can be seen in Fig. 4, the macropulse energy of the FEL is measured to be higher than 10 mJ at wavelengths around 70 μm, which is more than three times higher than that obtained in the 108 MHz mode. The number of micropulses in the 27 MHz mode is approximately 100, which is a quarter of that in the 108 MHz mode, so that the micropulse energy exceeds 0.1 mJ, which is ten times higher than the value obtained in the 108 MHz mode.

CHARACTERIZATION

The main parameters of the THz-FEL are listed in Table 1. The characteristics of the FEL have been measured, including detuning curves, wavelength spectra, macropulse structures consisting of many micropulses measured with fast THz detectors, time structures of micropulses using a Michelson interferometer, and so on. Two examples among them are shown below.

Figure 5 shows wavelength spectra of the FEL operated in the 108 MHz mode at the electron energy of 15 MeV and an optical cavity detuning for the maximum FEL gain by varing the wiggler gap in steps of 1 mm. The wavelength can be varied from 50 to 105 μm or from 2.9 to 6 THz for the fixed electron energy of 15 MeV. Another example is an interferogram shown in Fig. 6, which is measured for the micropulses in the 27 MHz mode operated at 15 MeV, the wiggler gap 30 mm, the wavelength 105 μm, and the zero-detuning position, where the macropulse energy is highest. The fine

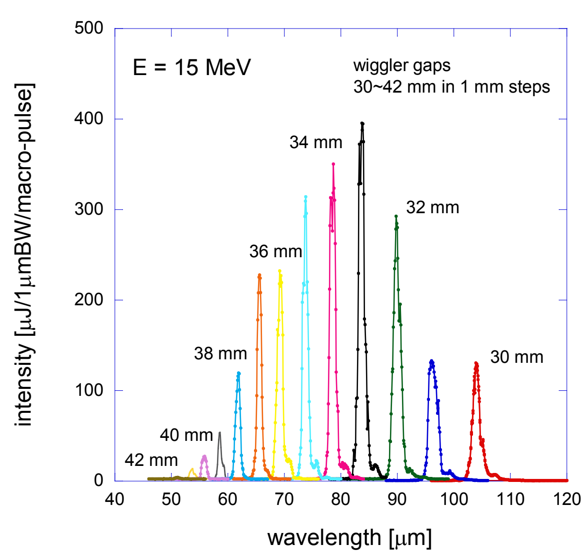

Figure 5: Wavelength spectra measured with a monochrometer in the conventional operation mode (108 MHz mode) of the FEL at the electron energy of 15 MeV by varying the wiggler gap.

Copyright © 2015 CC-BY-3.0 and by the respective authors

ISBN 978-3-95450-134-2

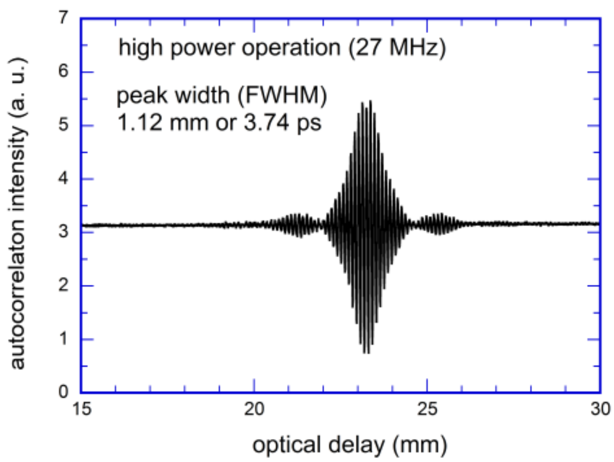

Figure 6: Autocorrelation pattern of FEL micropulses measured with a Michelson interferometer and an energy meter in the high power mode (27 MHz mode) at the electron energy of 15 MeV, the wiggler gap of 30 mm, and the zero detuning. The wavelength is 105 μm.

structure is due to interference of the monochromatic light, so that intervals of the interferences are a half of the wavelength 105 μm. The width of the interference peak is 1.12 mm or 3.74 ps. If it is assumed that the peak width is equal to twice the micropulse duration, though there are some discussions on interpretation of the interference pattern, the micropulse duration is estimated to be 0.6 mm or 2 ps.

APPLICATIONS

We began application experiments with spectroscopic and imaging studies using the THz-FEL. A Czerny-Tuner monochromator is used for spectroscopic studies. The wiggler gap for the FEL and the wavelength of the monochromator are synchronously scanned to measure a high resolution spectrum. Figure 7 shows an transmission spectrum of water vapor in the air measured with the FEL operated in the conventional mode and compared with a

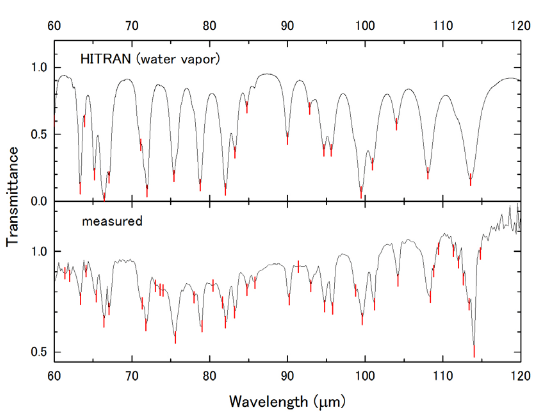

Figure 7: Transmission spectrum of water vapor in the air measured with the FEL in the conventional mode (lower panel) and calculated one of HITRAN (upper panel).

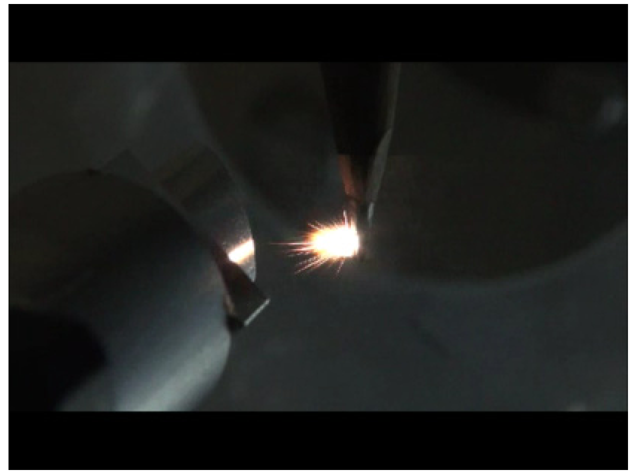

Figure 8: Spark generated by the FEL beam in the high power mode or the 27 MHz mode focused on the lead of a pencil using an off-axis paraboloidal mirror with a focal length of 12.5 mm.

calculation of HITRAN. The measure fine structures are in good agreement with the calculated ones. Another example is a wavelength resolved imaging by the raster method. The FEL is also used for measurement of characteristics of THz cameras conducted in collaboration with NEC Corporation [5].

In the high intensity operation of the FEL, the FEL beam can make aerial discharge and a plume on a pencil lead, as shown in Fig. 8, when it is focused with an off-axis paraboloidal mirror with a focal length of 12.5 mm. The peak power of the micropulse at a wavelength around 70 μm or 4.3 THz is calculated to be P = 50 MW for the micropulse energy 0.1 mJ and the duration of 2 ps. The FEL beam coming out through the window of the evacuated beam line to the experimental station is nearly circular and its size is measured to be $\sigma_r = 1.7$ mm (rms). When it is focused using the mirror with f = 12.5 mm, the focused beam radius is estimated to be 47 μm (rms) using the relation for diffraction-limited light, $\sigma_r \times \sigma_r' \sim \lambda/4\pi$, and the cross sectional area of the FEL beam at the focal point is calculated to be $S = \pi\sigma_r^2 = 7.0\times10^{-5}$ cm^2. Then the power density there is calculated as I = P/S = 0.7 TW/cm^2, from which the electric field and the magnetic field are calculated as

$$E\,[\mathrm{V/cm}] = 27.5\times\sqrt{I\,[\mathrm{W/cm^2}]} = 27\,[\mathrm{MV/cm}] \qquad (1)$$

$$B\,[\mathrm{T}] = E\,[\mathrm{V/m}]/c = 9\,[\mathrm{T}] \qquad (2)$$

Using this high intensity THz radiation, studies on various non-linear effects are being conducted in collaboration with some groups working on THz science and technology [6].

SUMMARY

The recent progress in development of the THz-FEL at ISIR, Osaka University was reported. Pulse-to-pulse fluctuations of FEL macropulse energy are reduced by upgrading the high voltage power supply and the

ISBN 978-3-95450-134-2

Copyright © 2015 CC-BY-3.0 and by the respective authors

introduction of the solid state switch for the klystron modulator. Application experiments have begun using the stable and intense THz beam.

ACKNOWLEDGMENT

A part of this work was supported by JSPS KAKENHI Grant Numbers 24310069 and 24651102.

REFERENCES

[1] R. Kato et al., Nucl. Instrum. Methods Phys. Res., Sect. A 429 (1999) 146.
[2] G. Isoyama et al., Infrared Phys. Technol. 51 (2008) 371.
[3] A. Tokuchi et al., Nucl. Instrum. Methods Phys. Res., Sect. A 769 (2015) 72.
[4] S. Suemine et al., Nucl. Instrum. Methods Phys. Res., Sect. A 773 (2015) 97.
[5] N. Oda et al., Proc. of SPIE Vol. 9102 910202, (5-6 May 2014, Baltimore, Maryland, USA).
[6] M. Nagai et al., Proc. of IRMME-THz 2014, (14-19 September 2014, Zcson, Arizona, USA), IEEE 10.1109/IRMMW-THz.2014.6956352.

Copyright © 2015 CC-BY-3.0 and by the respective authors

ISBN 978-3-95450-134-2